Journal of Membrane Science 514 (2016) 467–475

Contents lists available at ScienceDirect

Journal of Membrane Science

journal homepage: www.elsevier.com/locate/memsci

Development of oxygen and temperature sensitive membranes using molecular probes as ratiometric sensor

S. Santoro, A.J. Moro, C.A.M. Portugal, J.G. Crespo, I.M. Coelhoso, J.C. Lima *

LAQV, REQUIMTE, Departamento de Química, Faculdade de Ciências e Tecnologia, Universidade Nova de Lisboa, 2829-516 Caparica, Portugal

ARTICLE INFO

Article history:
Received 23 October 2015
Received in revised form
23 April 2016
Accepted 3 May 2016
Available online 12 May 2016

Keywords:
Molecular probes
Fluorescence
Oxygen sensitive membranes
Temperature sensitive membranes
Ratiometric sensor
Temperature correction

ABSTRACT

In this work we show that, the combination of (i) high mechanical stability (provided by a PS matrix), (ii) high sensitivity and selectivity (provided by a two-dye system of Tris (1,10-phenanthroline)ruthenium(II) chloride hydrate ($Ru(phen)_3$) and 7-Methoxy-4-methylcoumarin) and (iii) high reproducibility in the output signal/response, results in a membrane able for monitoring O_2 and temperature in membrane processes at laboratory and industrial scales.

Due to the matched sensitivity of the developed ratiometric probe to oxygen and temperature a simple correction algorithm was implemented, which allows at overcoming the vulnerability of the ratiometric signal to the temperature, leading to a robust evaluation of the oxygen concentration.

The impact of introducing this photochemical activity in membranes opens a new perspective for non-invasive monitoring of membrane processes (e.g. measurement of temperature in membrane distillation processes, oxygen measurement for monitoring of biofilm onset and development in reverse osmosis).

1. Introduction

Membrane processes are governed by physical-chemical interactions between the boundary layer of the solutions in contact with the membranes and the membrane surfaces [1]. Efforts in membrane science have been devoted to the development of innovative materials and optimization of operating conditions in order to maximize the selective permeant-membrane interactions, increasing the performance of the process in terms of productivity, selectivity and stability [2]. Moreover, it is notorious that these interactions dynamically change at the membrane surface due to variations of the operating conditions and membrane properties related to phenomena such as the concentration and/or thermal polarization, fouling, swelling and membrane deterioration [2–6].

Nowadays, common analytic technologies are used for the monitoring of the global performance of the process, estimating the permeability and the selectivity of the membrane and evaluating the long-term stability of the separation process. Oxygen (O_2) and temperature (T) are two fundamental parameters affecting every chemical and biological process, including membrane processes and electrochemical sensors, such as thermocouple for temperature monitoring and Clark electrode for detection of oxygen levels (yO_2), are used as accurate and inexpensive technologies with a rapid response time [12–13]. However, the miniaturization of the sensors is critical for some applications in innovative research fields [14–18] and industrial processes [19–22].

Even with miniaturized approaches, there is still a gap in providing real-time information at the micron and submicron scale about the phenomena occurring in the permeant-membrane interface with impact in the global process, i.e., in-situ real-time monitoring of membrane processes, operating at a molecular scale [7].

The immobilization of luminescent molecular probes in/onto polymeric matrices, is an attractive technology for non-invasive monitoring, allowing to obtain functional materials with a continuous response to temperature changes and/or oxygen content [8] at micrometric and sub-micrometric scale [9,10] with a short response time [11].

The performance of the functional material to be used as an optical sensing device will strongly depend on the fundamental properties of the polymer (e.g. oxygen permeability, transparency, mechanical stability) [23] and the fluorescent probe (e.g. quenching efficiency by oxygen and/or temperature, long term stability) but also on the operating conditions (changes on the geometry of the optical setup, fluctuations of the excitation source, inhomogeneous probe concentration distribution).

In general, polymers with high oxygen permeability, such as poly(dimethylsiloxane) (PDMS), are employed in oxygen sensing, however, a rigid support is often required [24] due the lack of mechanical stability. Furthermore, poor solubility of luminescent

* Corresponding author.
E-mail address: lima@fct.unl.pt (J.C. Lima).

http://dx.doi.org/10.1016/j.memsci.2016.05.019
0376-7388/

probes in silicone resins can lead to inhomogeneous dispersion of the molecules and self-quenching effects [13]. On the other hand, glassy polymers such as polystyrene (PS), present a reasonable oxygen permeability and good mechanical properties which allow the preparation of self-consistent films, with improved versatility [24,25].

Several works in the literature are devoted to the development of luminescent probes with high sensitivity to oxygen and long term stability [26–29]. Luminescent transition metal polypyridyl complexes and metalloporphyrins have been widely employed [29]. In particular, Ru(II) polypyridyl complexes present unmatched photostability despite they suffer from pronounced cross talk between oxygen and temperature sensing, since their triplet states are subjected to severe thermal quenching. Strategies like the immobilization of the molecular probes in polymers with low oxygen permeability such as polyacrylonitrile [30] were employed to produce temperature sensing materials insensitive to oxygen. It is thus a common limitation of optical sensors based on fluorescence (or phosphorescence) quenching by oxygen, that both the emission intensity and the excited state life time, are affected by temperature [31,32].

A strategy to overcome these drawbacks is the simultaneous use of two luminescent probes dispersed in the same polymeric matrix, which allow the combination of their emission intensities in a ratiometric signal, for the correction of errors produced by the fluctuations of the operative conditions [33–35].

In the present work Tris(1,10-phenanthroline)ruthenium(II) ($Ru(phen)_3$), a luminescent transition metal polypyridyl complex, was used as oxygen sensitive probe. The performance of polystyrene (PS) and poly(β-hydroxybutyrate-β-hydroxyvalerate) (PHBV) membranes as the solid matrices for the fluorescence sensor was evaluated. The ratiometric response was achieved through the co-dispersion of a second fluorophore insensitive to oxygen: 7-Methoxy-4-methylcoumarin, Dansyl Chloride and Quinine Sulfate were evaluated.

Finally, a correction model was implemented to compensate temperature drifts along the operation of monitoring O_2 concentration. This strategy yields a response to oxygen concentration which is independent from temperature, optical setup, fluctuations in the excitation light intensity and changes in transmission properties of the membrane, providing a way to accurately monitor O_2 levels at laboratory and real case situations.

The impact of introducing this photochemical activity to membranes opens a new perspective for non-invasive monitoring of membrane processes (e.g. mapping of the temperature on membrane surfaces during membrane distillation processes, oxygen measurement for monitoring of biofilm onset and development in reverse osmosis).

2. Materials and methods

2.1. Materials

Polystyrene (PS, M_w=192,000) was purchased from Sigma Aldrich Chemistry (Spain), whereas Poly(3-hydroxybutyrate-*co*-3-hydroxyvalerate) (PHBV, M_w=300,000) containing 3 mol% of 3-hydroxyvalerate units was obtained from Tianan Biologic Material Co. Ltd. (China). Tris(1,10-phenanthroline)ruthenium(II) ($Ru(phen)_3$) was synthesized according to the procedure reported in the literature [36]. The other molecular probes 7-methoxy-4-methylcoumarin (Coumarin), Dansyl Chloride and Quinine hemisulfate salt monohydrate (Quinine Sulfate) and the solvent (Chloroform) were purchased from Sigma Aldrich Chemistry (Spain).

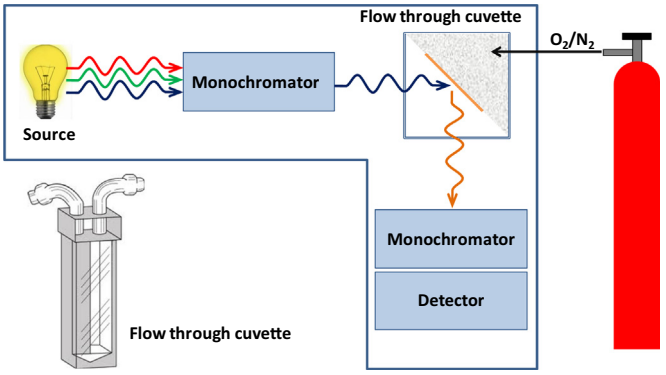

Fig. 1. Scheme of the spectrofluorometer and cuvette used for preliminary experiments.

2.2. Methods

2.2.1. Fluorescence measurements

Fluorescence measurements were performed with a Horiba-Jobin-Yvon SPEX Fluorolog 3.22 spectrofluorimeter equipped with a 450 W Xe lamp. All spectra were collected with a 5 nm slit bandwidth for excitation and emission and corrected.

Preliminary tests for the selection of the materials and evaluation of the response of the membranes to the oxygen level were performed using a flow through cell (10 mm optical path) with inlet/outlet tubes which allow a constant flow of gas. The optical sensing membrane was placed on the surface of a triangular prism made of porous glass in order to establish an angle of 45° between excitation and emission light while allowing for non-hindered gas transport trough the membrane (Fig. 1).

The two-dye ratiometric sensing membranes response to oxygen concentration and temperature was characterized with the setup depicted in Fig. 2. The sensing membrane was mounted in a steel cell with a quartz window. A bifurcated optical fiber bundle, in contact with the quartz window, transports the excitation light and collects the emission of the membrane, while the emission spectrum is registered by a spectrofluorimeter. Mixtures of oxygen/nitrogen with different oxygen concentrations (0%, 10%, 21%, 50% and 100% v/v) purchased from Praxair (Spain) were fed to the cell that was subsequently sealed using two valves (Fig. 2). The pressure of the cell during the experiments was kept at 1 atm. The area of the optical sensing membrane was 1 cm^2. The distance between the optical fiber and the membrane was 1.5 cm. The chamber was kept at constant temperature, which was varied from 25 °C to 50 °C to study the effect of temperature.

2.2.2. Membrane preparation

The membranes were prepared by dry-casting a dope solution of polystyrene (PS) solubilized in 10 ml of chloroform (25 w/v%).

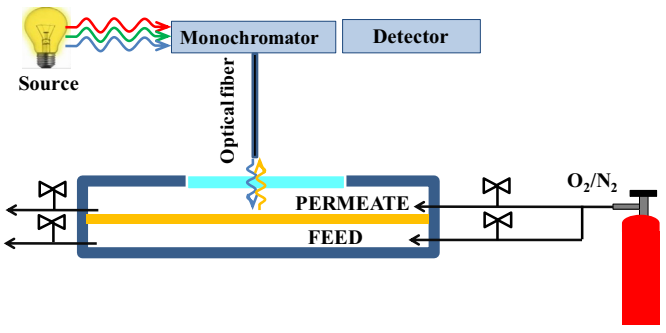

Fig. 2. Scheme of experimental set-up used for evaluation of probe sensitivity to oxygen and temperature.

After total dissolution of the polymer (after stirring the solution at 30 °C overnight) 1 ml of chloroform containing the fluorophores (ranging from 10^{-3} M to 10^{-5} M) was added to the polymeric solution. The amount of fluorophore (with respect to the mass of polymer) was varied from 8×10^{-7} mol g^{-1} to 8×10^{-9} mol g^{-1}. In the case of the ratiometric two-dye system a second injection of 1 ml of chloroform containing the reference (Coumarin, Quinine Sulfate or Dansyl Chloride) was also performed. The concentration of the reference was equal to the concentration of the oxygen sensitive luminescent probe, except for Dansyl Chloride which was one order of magnitude higher.

In order to assure homogeneous dispersion of the fluorophores in the polymer matrix, the dope solution was stirred for 2 h and sonicated for 1 h. Then, the polymeric solution was cast using a casting knife with a thickness of 0.75 mm. After evaporation of the solvent at room temperature (ca. 48 h), the membranes prepared were placed in an oven at 65 °C over night in order to favor the removal of solvent traces, generating membranes with thicknesses of 144 ± 3 μm.

The procedure for the preparation of the PHVB membranes was similar. In this case total dissolution of the polymer pellets in chloroform was achieved by heating the polymeric solution at 60 °C for 90 min

2.2.3. Physical characterization of the membranes

The membranes' morphology was observed in scanning electron microscopy (Quanta FEG 250). Membranes cross sections were prepared by freeze fracturing the samples in liquid nitrogen, to produce a clean brittle fracture. Thermogravimetric analyses were performed using a Mettler Toledo TGA/SDTA 851e equipment.

Gas permeation of N_2, O_2, and CO_2, at a constant temperature of 25 ± 1 °C, were performed using a fixed volume/pressure increase instrument [37], manufactured by GKSS (Geesthacht, Germany). Evaluation of the diffusion coefficient, solubility and permeability of gases through the PS membrane (with and without fluorophores) was performed.

3. Results and discussion

3.1. Oxygen sensitive membrane

$Ru(phen)_3$, known as a phosphorescent molecule with long lived luminescence and good oxygen sensitivity [25] was tested as a potential oxygen sensitive probe in the preparation of oxygen sensitive membranes at a concentration of 8×10^{-7} mol g^{-1} in PS. The emission spectra of the probe immobilized in PS in degassed (0% oxygen) and aerated (21% oxygen) conditions, together with the background emission spectrum of bare PS, are reported in Fig. 3. The emission was collected exciting the membrane at the maximum of absorption of the Ruthenium complex in PS (459 nm). $Ru(phen)_3$ showed its maximum emission at 589 nm and it is clearly distinguishable from the background luminescence of PS.

As reported in Fig. 3, the intensity of the emission of $Ru(phen)_3$ increased 20% as a consequence of the decrease of the oxygen concentration from 21% to 0% (v/v).

3.2. Optimization of the oxygen sensitive membrane

Ruthenium loaded membranes were produced with different probe concentrations and different polymeric matrices. Fig. 4a reports the effect of the concentration of $Ru(phen)_3$ on the polymeric membrane emission intensities in the case of PS.

The intensity of the peak at 589 nm increased by increasing the

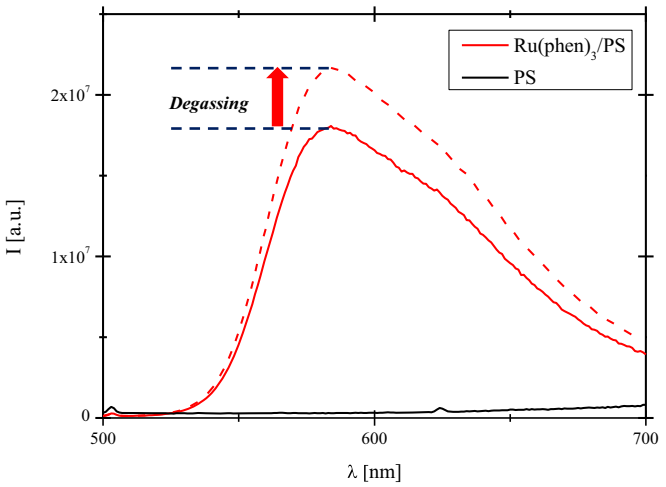

Fig. 3. Effect of the oxygen concentration on the emission spectra of $Ru(phen)_3$ (b) immobilized in PS films (T=21 °C, probe concentration 8×10^{-7} mol g^{-1}). Experiments were performed using the set-up shown in Fig. 1.

amount of $Ru(phen)_3$, as predicted by the equation:

$$I = k I_{exc} \Phi [\varepsilon b c] \quad (1)$$

where I_{exc} is the intensity of the exciting light, ε and c are respectively the molar extinction coefficient and the concentration of the luminophore and b is the optical path. This linearity is a clear sign of absence of probe aggregation at the concentrations used.

The ratio of the emission intensity (collected at the emission band maximum) of $Ru(phen)_3$ in the absence of oxygen (I_0) and the emission intensity at the different oxygen concentrations (I) is represented for different oxygen concentrations in Fig. 4b. For all concentrations tested, the I_0/I ratios show the linear dependence with oxygen concentration expected from the well-known Stern-Volmer linear equation:

$$I_0/I = 1 + K_{SV} [O_2] \quad (2)$$

A slight increase in sensitivity was observed upon increasing $Ru(phen)_3$ concentration in the membrane, which is probably due to the increase of the signal-to-noise ratio at higher concentrations. Nevertheless, a 100-fold increase in probe concentration only results in 1.5-fold increase in sensitivity.

The response of the sensing membrane to oxygen concentration can be tuned by the oxygen permeability of the polymer matrix where the fluorophore is dispersed. Thus, the sensitivity to oxygen was evaluated for $Ru(phen)_3$ dispersed in two different polymeric matrices with different oxygen permeability coefficients. PS, which combines a reasonable oxygen permeability with good mechanical properties consenting to prepare a self-consistent device, and PHBV, a biopolymer of low environmental impact and lower oxygen permeability, were employed [38,39]. The amount of the probe dispersed in both polymeric matrices was 8×10^{-7} mol g^{-1}.

The comparison of the performance of the two polymers can be made from the respective Stern-Volmer plots shown in Fig. 5. The sensitivity of the sensor prepared using PS is ca. 3 times higher than that observed for the probe dispersed in PHVB. This can be partially attributed to the higher oxygen permeability in PS. The sensitivity of the optical sensor is expected to follow the equation:

$$I_0/I = 1 + \frac{4\alpha\pi N_A \sigma}{1000} \tau_0 P(O_2) p(O_2) \quad (3)$$

where N_A is Avogadro's number, σ is the collision radius of the oxygen-probe complex, $p(O_2)$ is the oxygen partial pressure and

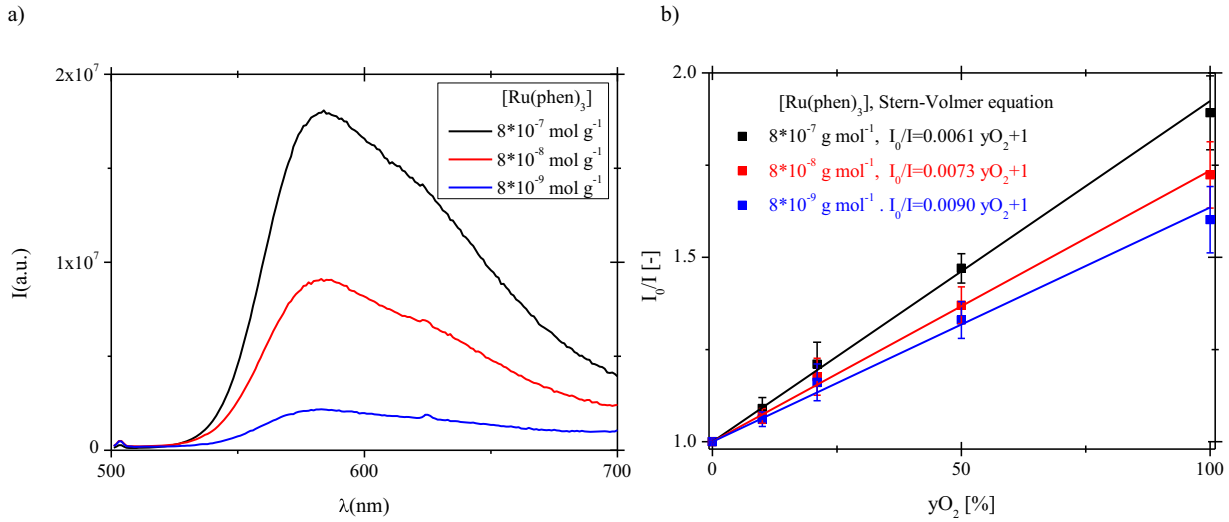

Fig. 4. Effect of the concentration of Ru(phen)$_3$ on the emission intensity at 21% O_2 (a) and on the slope of the Stern-Volmer plot against oxygen concentration (b) (T=21 °C). Experiments were performed using the set-up shown in Fig. 1.

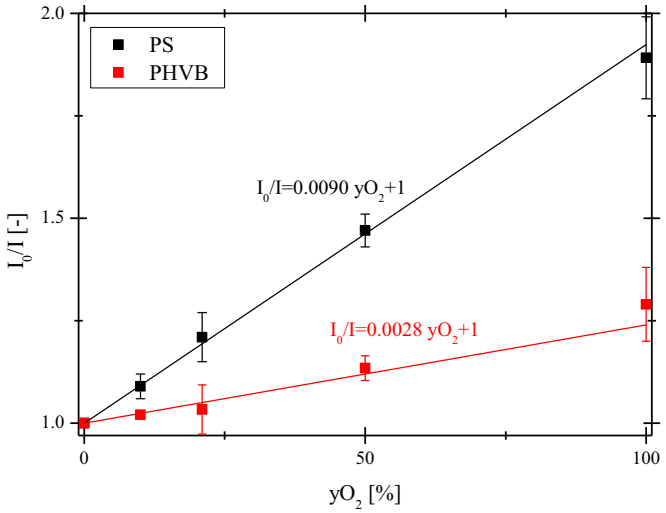

Fig. 5. Stern-Volmer plots obtained for membranes prepared with PS and PHVB (T=21 °C, probe concentration 8×10^{-7} mol g^{-1}). Experiments were performed using the set-up shown in Fig. 2.

$P(O_2)$ is the oxygen permeability in the polymer which is 0.34 barrer (2.8×10^{-13} m^2 s^{-1}) for PHVB and 3.6 barrer (3.0×10^{-12} m^2 s^{-1}) in the case of PS [38,39].

The ca. 10 times increase in the permeability to oxygen when going from PHVB to PS is not accompanied by an equivalent change in sensitivity (only ca. 3 times increase). The most straightforward explanation resides in the differences of the emission decay times (τ_0) of Ru(phen)$_3$ when dispersed in the different polymers.

3.3. Development of a ratiometric sensor based on ruthenium

The emission of the oxygen sensor based on Ru(phen)$_3$ is prone to variation of operating conditions (i.e. oxygen level, optical setup, chromophore concentration, intensity of excitation light, temperature) limiting the robustness of the oxygen detection. To overcome this limitation a second fluorescent molecule non-sensitive to oxygen (reference) was added to the membranes in order to develop a ratiometric sensor. Using this additional probe it is expected to improve the robustness of the measurements by discrimination of the emission changes exclusively attributable to O_2 concentration differences. The ideal reference probe is required to have a well discernible emission from Ru(phen)$_3$ and low sensitivity to oxygen. Three different fluorophores complying with the mentioned requisites were evaluated: Quinine Sulfate, Dansyl Chloride and Coumarin.

Both the membranes prepared with Coumarin and Quinine Sulfate, as reference fluorophores, have shown two perfectly discernible bands (see Table 1; emission maximum of Ru(phen)$_3$ is at 589 nm) with more than 100 nm separation between the emissions of reference and sensing dyes. Also both Coumarin and Quinine Sulfate emissions are not significantly affected by oxygen concentration ($I_{0\%}/I_{21\%}$=1.02 for Coumarin and $I_{0\%}/I_{21\%}$=0.97 for Quinine Sulfate); whereas those ascribed to Ru(phen)$_3$ increased by decreasing the oxygen level, as previously described. On the other hand, the intensity of Dansyl Chloride is strongly overlapped with the emission of Ru(phen)$_3$ and moreover there are significant emission intensity changes upon oxygen removal ($I_{0\%}/I_{21\%}$=1.28), limiting its employment as a reference.

The ratiometric response, R, is obtained dividing, for any oxygen concentration, the intensity collected at the maximum of the reference emission band by the emission collected at the maximum of Ru(phen)$_3$ emission:

$$R = I_{Reference}/I_{Ru(phen)_3} \quad (4)$$

The change of the ratiometric reponses upon change in oxygen concentration are a measure of the two-dye ratiometric system sensitivity to O_2 (see Table 1). The ratiometric response to oxygen removal ($R_{0\%}/R_{21\%}$) is 1.24 in the case where Coumarin is used as reference and 1.03 in the case where Quinine Sulfate is used as reference. For the reasons stated above Coumarin performs best as a reference dye in the ratiometric sensing membranes.

Table 1
Comparison of the emissive properties of the reference dyes in the ratiometric sensors: wavelength of emission (λ); intensities of emission in aerated conditions ($I_{21\%}$); ratio of emission intensities in degassed and aerated conditions ($I_{0\%}/I_{21\%}$); ratio of emissions of reference over Ru(phen)$_3$ collected at the respective maxima ($R_{21\%}$; at atmospheric pressure); sensitivity of the ratiometric response ($R_{0\%}/R_{21\%}$) to oxygen removal.

Reference probe	λ[nm]	$I_{21\%}$ [10^6 a.u.]	$I_{0\%}/I_{21\%}$	$R_{21\%}$	$R_{0\%}/R_{21\%}$
Coumarin	363	8.4	1.02	1.38	1.24
Quinine Sulfate	403	9.1	0.97	1.01	1.03
Dansyl Chloride	506	2.7	1.28	0.35	1.17

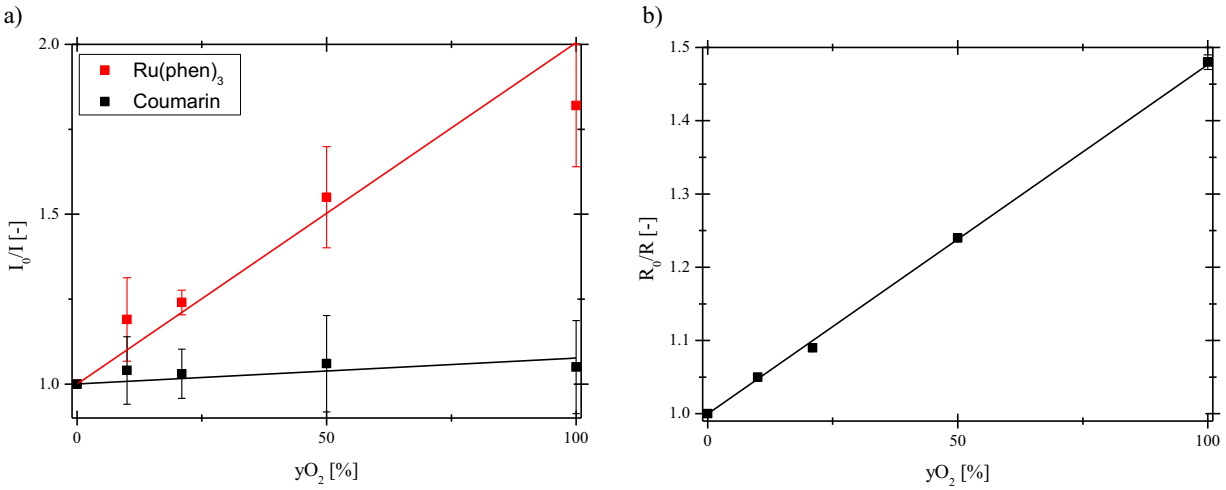

Fig. 6. Oxygen sensitivity at T=21 °C of (a) the intensities of emission of $Ru(phen)_3$ and Coumarin in PS and (b) the ratiometric signal. Experiments were performed using the set-up shown in Fig. 2.

3.4. Performance of the two-dye ratiometric membrane sensor for oxygen

The PS membrane containing equimolar amounts of Coumarin and $Ru(phen)_3$ was tested using the set-up reported in Fig. 2. The oxygen concentration in the cell was varied from 0% to 100%. Experiments were performed using 2 different samples in order to evaluate the reproducibility of the response. The results obtained are summarized in Fig. 6, where the Stern-Volmer plots of the $Ru(phen)_3$ emission intensities, (I_0/I, Fig. 6a) and intensity ratios (R_0/R, Fig. 6b, $R=I_{Coumarin}/I_{Ru\,(phen)_3}$) are put together for comparison. The high experimental errors and the relatively low value of the correlation factor (0.922) of the linear plot of Fig. 6a, are a clear evidence of the negative impact of small fluctuations of operating conditions on the sensor performing with a single probe. On the other hand, the intensity ratios not only show the same linear increase with oxygen concentration, but also the correlation factor becomes higher than 0.99. The associated error lowers to around 1%, due to the cancellation of errors resulting from the ratio of signals.

The ratiometric signal robustness can be better understood by the observation that combining Eqs. (1) and (4), and considering that the PS membranes contain an equimolar amount of the two probes, the ratio of the probes' intensities can be given by the equation:

$$\boldsymbol{R}=(\boldsymbol{\Phi\varepsilon})_{\boldsymbol{Coumarin}}/(\boldsymbol{\Phi\varepsilon})_{\boldsymbol{Ru\,(phen)_3}} \quad (5)$$

that depends only on the photophysical properties (quantum yield and extinction coefficients) of the two dyes.

Since Coumarin is non-sensitive to oxygen, we can assume that the linear response of the ratiometric probe to the oxygen level is the Stern-Volmer constant which expresses the dynamic quenching of the ruthenium complex. It is important to stress out that transition-metal complexes, in particular immobilized in silicone rubber, often do not exhibit perfectly linear Stern-Volmer calibration plots due to the presence of micro heterogeneities within the polymer [40]. The performance of the PS/$Ru(phen)_3$/Coumarin membranes towards sensing are in this case remarkable, showing linearity in the whole range of oxygen concentrations (from 0% to 100%), which is an evidence of the sensor structural and chemical homogeneity.

Additionally, SEM analyses showed that the morphology and the thickness of the PS membrane is not affected by addition of the molecular probes at the low concentrations used in this study (Supplementary Material). The amount of probe is so low that it was not possible to detect the presence of atomic Ruthenium by analysis of energy-dispersive X-ray microanalysis (EDS). The PS membrane containing $Ru(phen)_3$ and Coumarin presents a symmetric dense morphology comparable with that observed in the membrane of bare PS. Also thermogravimetric analysis (TGA) shows that doped PS and the pure polymer are identically stable. In fact, in both cases, degradation occurs in the range of 350–420 °C and the melting point was evaluated at 398 °C (Supplementary material).

Regarding the permeability measurements (Table 2), PS is a glassy polymer with moderate gas permeability. The most permeable species is carbon dioxide, whereas O_2 shows a moderate permeability due to the combination of a high diffusion and low solubility. The immobilization of the molecular probes in the polymeric matrix did not affect significantly the barrier properties of the PS membrane.

In summary, the pristine functionality of the membrane is not affected by the presence of the low concentration of the dyes, while the two-dye system confers to the membrane an additional O_2 sensing functionality of superior performance (full range linearity and very low error).

Table 2
Permeability, diffusion coefficient and solubility of different gases in the membranes of PS and PS doped with $Ru(phen)_3$ and Coumarin. [Probe]=8×10^{-7} mol g^{-1}.

	PS			PS/Ru $(phen)_3$/Coumarin		
Gases	O_2	N_2	CO_2	O_2	N_2	CO_2
P [barrer]	2.34 ± 0.12	0.35 ± 0.02	13.09 ± 0.65	2.47 ± 0.12	0.42 ± 0.02	12.24 ± 0.61
D [10^{-12} m^2 s^{-1}]	12.05 ± 0.63	4.08 ± 0.21	5.26 ± 0.26	10.02 ± 0.51	3.57 ± 0.18	4.14 ± 0.21
S [cm^3(STP) cm^{-3} bar^{-1}]	0.15 ± 0.01	0.06 ± 0.01	1.87 ± 0.09	0.19 ± 0.01	0.09 ± 0.01	2.22 ± 0.11

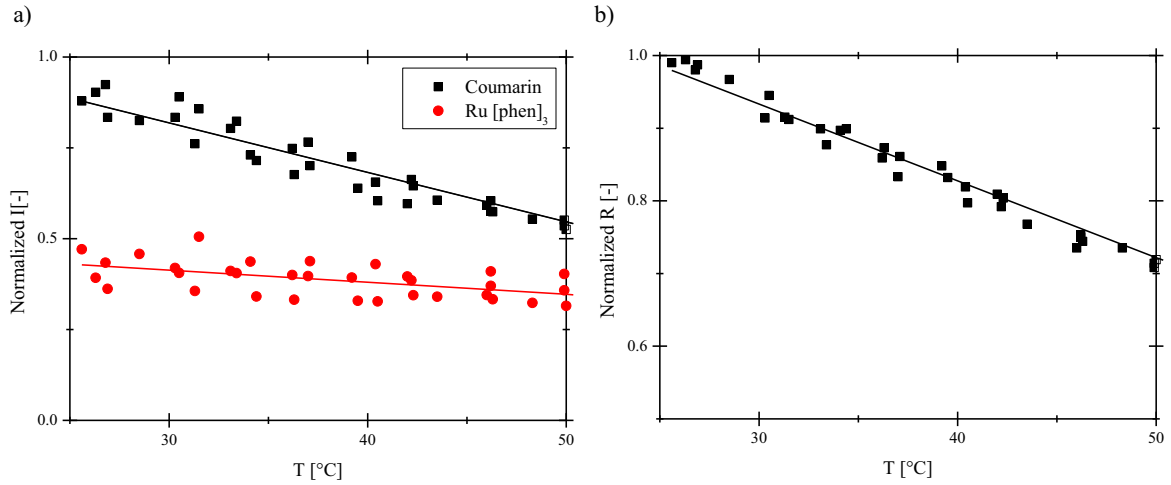

Fig. 7. Effect of the temperature on (a) the intensities of the emission of $Ru(phen)_3$ and Coumarin in PS and (b) the ratio of their intensities, recorded at yO_2=21%.

3.5. *Temperature sensitivity of the two-dye ratiometric membrane*

The use of the two probes and the combination of their emission in a ratiometric signal allows for the development of a robust sensor for measurement of oxygen level. However, it is ubiquitous that fluorescent probes also respond to temperature, and in "out-of-lab" applications the increase in temperature will lead to a decrease in fluorescence intensities of both probe and reference dyes that can lead to underperformance at very high temperatures. On the other hand, under controlled oxygen atmosphere, the two-dye ratiometric membrane can also perform as a thermometer.

The effect of temperature on the sensor and reference emission intensities, when exposed at constant atmospheric pressure (yO_2=21%) are shown in Fig. 7a while the ratio of the reference over sensor intensities is presented in Fig. 7b.

The emission intensities of both fluorophores decrease with the increase of the temperature (Fig. 7a), however, Coumarin emission decreases 45%, whereas $Ru(phen)_3$ emission decreases only 20%, upon increasing temperature from 25 °C to 50 °C. As a consequence of the different sensitivity of the two probes towards temperature, the ratio of intensities of their emissions decreases by increasing the temperature. Again, the single probe emissions are much more affected by fluctuations in operation conditions (Fig. 7a) while the ratio of the emission intensities (R) allows for an accentuated error reduction (< 3%) and a decrease of 30% of the normalized ratio ($R/R_{25\ °C}$) was obtained after increasing the temperature from 25 °C to 50 °C at a constant oxygen concentration (yO_2=21%).

3.6. *Matched sensitivity to oxygen and temperature*

The simultaneous impact of temperature and oxygen in the emission hampers the simultaneous determination of both parameters by the sensing membrane. Also, changes in the operating conditions such as temperature will have a negative impact in the accuracy of oxygen concentration determination by the sensing membrane. In Fig. 8, it is possible to observe the crosstalk of the temperature and oxygen on the luminescent response of the membrane.

The ratiometric response linearly increases by increasing oxygen at any temperature as a consequence of the quenching of $Ru(phen)_3$ (Fig. 8a), while the effect of temperature is to favor the non-radiative deactivation of both Coumarin and $Ru(phen)_3$, decreasing the value of the ratio of their intensity for a given oxygen concentration (Fig. 8b). A single point measurement to determine the oxygen concentrations requires the knowledge of the exact temperature and vice versa.

Furthermore, the increase of temperature decreases the oxygen sensitivity of the membrane, as can be evaluated by the decrease in the Stern-Volmer constants, K_{SV} (slopes of the Stern-Volmer type representations of the intensity ratios, R_0/R) (Fig. 9a). The increase of oxygen concentration also decreases the thermal

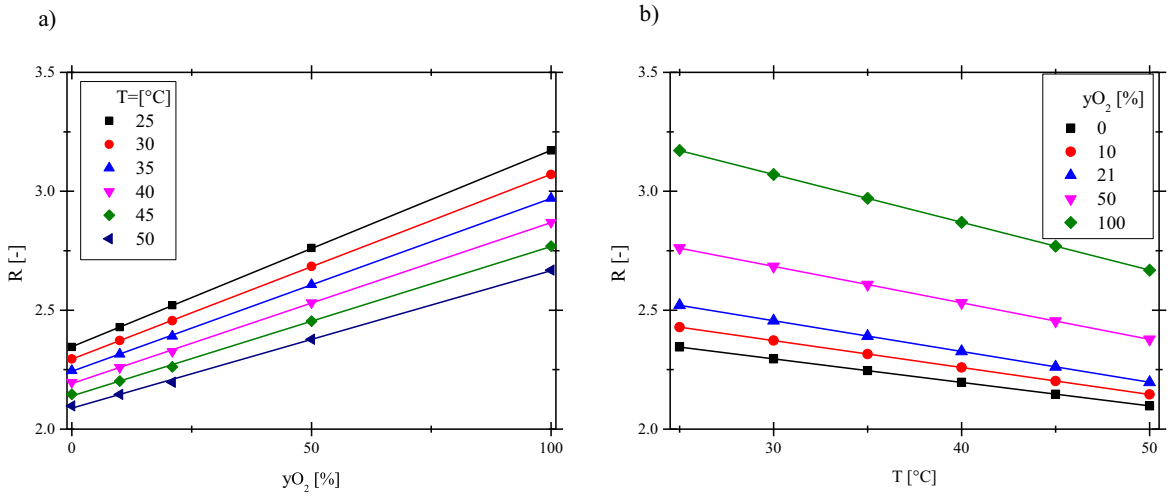

Fig. 8. Effect of temperature on oxygen sensitivity (a) and of oxygen on temperature sensitivity (b). Experiments were performed using the set-up shown in Fig. 2.

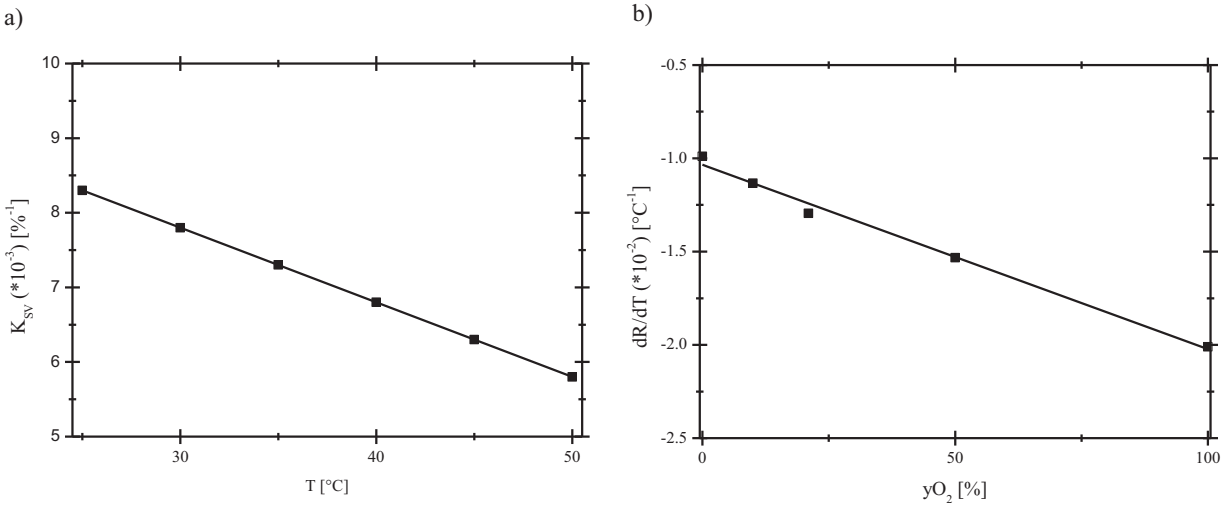

Fig. 9. Effect of temperature on the Stern-Volmer constant (slope) (a) and of oxygen on the temperature sensitivity (b).

sensitivity of the dual emission of the membrane (Fig. 9b) as evaluated by the slopes of the ratio (R) of intensities with respect to temperature.

3.7. Temperature compensation of the oxygen sensor

Lo et al. [41] developed a simple model for evaluation of oxygen concentration, non-dependent from temperature, using the emissive complex platinum(II) *meso*-tetrakis(pentafluorophenyl) porphyrin (PtTFPP). The model developed allowed them to evaluate the temperature compensation C(T) for the sensor response using the emission intensity of the complex.

The same model was applied to the emission ratios obtained in this work, (R), according to Eq. (6):

$$\boldsymbol{C}(\boldsymbol{T}) = \frac{\boldsymbol{R}_0(\boldsymbol{T}_{ref})}{\boldsymbol{R}(\boldsymbol{T})} - \frac{\boldsymbol{R}_0(\boldsymbol{T}_{ref})\boldsymbol{f}_1\boldsymbol{K}_{SV}(\boldsymbol{T}_{ref})\boldsymbol{yO}_2}{\boldsymbol{R}(\boldsymbol{T})\{1+\boldsymbol{K}_{SV}(\boldsymbol{T}_{ref})\boldsymbol{yO}_2\}}; \quad (6)$$

where $R_0(T_{ref})$ is the ratio of intensities in the absence of oxygen at the reference temperature (T=25 °C), and R(T) is the ratiometric response at a certain oxygen level and temperature of the measurement, $K_{SV}(T_{ref})$ is the Stern–Volmer constant at the reference temperature (T=25 °C) for the ratiometric sensor and f_1 is the fractional intensity of the component contributing to the total luminescence at the given temperature of the measurement (it is assumed to be 1 since no deviation from linear Stern-Volmer equation was observed, as already pointed out in Section 3.4).

The temperature insensitive ratio, R_m, was determined by Eq. (7).

$$\boldsymbol{R}_m = \boldsymbol{C}(\boldsymbol{T})\boldsymbol{R}. \quad (7)$$

Experiments were performed at different temperatures ranging from 25 °C to 50 °C and distinct oxygen concentrations (yO_2=0%, 21%, 50% and 100%) for evaluation of the temperature compensation effect. It was observed that the ratiometric response obtained in the whole range of temperatures follows a Stern-Volmer behavior ($R^2 > 0.99$). As stated above and clearly seen in Fig. 10. a the sensitivity of R_0/R signal to $y(O_2)$ decreases with the increase of temperature. This effect is clearly visible by the decrease of the R_0/R signal *vs.* $y(O_2)$ slope, as well as by the linear decrease of the ratiometric sensor Stern-Volmer coefficient at increasing temperatures.

According to Eq. (6), the value of the temperature compensation factor C(T) depends on the temperature and oxygen concentration. The temperature insensitive ratiometric signal, R_{m0}/R_m, was obtained after correction of R_0/R values using Eq. (7). The sensitivity of R_{m0}/R_m vs. yO_2 (%) is plotted in Fig. 10b. The parameter R_{m0}/R_m exhibits a good sensitivity to yO_2 without the

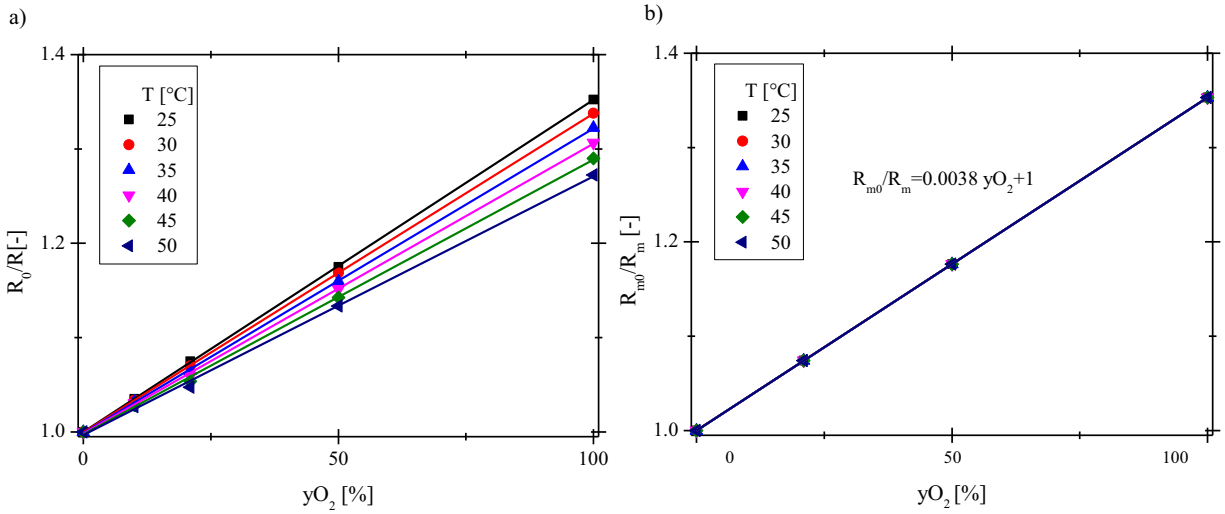

Fig. 10. (a) Effect of temperature on the Stern-Volmer ratiometric response and (b) Stern-Volmer compensated ratiometric response at different temperatures.

influence of temperature (the Stern-Volmer plots obtained at different temperatures are perfectly overlapped), yielding robust oxygen concentration readings not affected by changes in operation conditions.

4. Conclusions

In this work oxygen and temperature sensitive membranes were developed. The fluorescent membrane was based on the use of the $Ru(phen)_3$ as a molecular probe for oxygen monitoring. Studies confirmed that the sensitivity of the sensor increased by employing polymer matrices with high oxygen permeability, but, changes in the photophysical properties of $Ru(phen)_3$ induced by the polymer (e.g. excited state decay time) can have significant impact in the sensitivity. Also, the detection based on a single luminescent probe suffers of inaccuracy related to the optical setup and excitation geometry drifts. In order to correct for this Coumarin was selected as a reference due to the well discernible emission band and low oxygen sensitivity. The employment of a reference probe allowed to correct artifacts induced by fluctuations in the excitation light intensity, excitation geometry and optical path. The ratiometric sensor showed a linear response in the whole range with a sensitivity of $R_{100\%}/R_{0\%} \sim 1.5$ at room temperature (21 °C).

As expected, the ratiometric optical sensor was found to be sensitive to temperature. In fact, the ratiometric response decreased 30% by increasing the temperature from 25 °C to 50 °C. However, temperature compensation of the signal consents to calibrate the ratiometric optical sensor, thus obtaining a response independent from temperature, the optical path, excitation geometry and fluctuations in the excitation light intensity of the source and/or transmission properties of the optical fiber and membrane sensor. The reproducibility of the measurements in the range 25–50 °C is highlighted by the low error in oxygen level determination (0.1%) throughout the whole O_2 concentration range.

Given the combination of (i) high mechanical stability (provided by the PS matrix), (ii) high sensitivity and selectivity (provided by the two-probe system) and (iii) high reproducibility in the output signal/response, this membrane represents a significant step for monitoring O_2 and temperature in membrane processes. On-going work envisages the application of the developed membrane for monitoring of oxygen permeation in food packaging, for monitoring of temperature on PVDF membrane surfaces and for evaluation of thermal polarization in membrane distillation processes.

Acknowledgements

Sergio Santoro would like to thank The Education, Audiovisual and Culture Executive Agency (EACEA) for the Ph.D. grant under the Program “Erasmus Mundus Doctorate in Membrane Engineering” – EUDIME (FPA 2011-2014, http://www.eudime.unical.it). Artur Moro and Carla A, M, Portugal acknowledge the financial support of “Fundação para a Ciência e Tecnologia” through the Post-Doc grants nrs. SFRH/BPD/69210/2010 and SFRH/BPD/103619/2014, respectively.

The authors acknowledge the Institute on Membrane Technology for offering access to their instruments and expertise for measurements of gas permeability.

This work was also supported by the Associated Laboratory for Sustainable Chemistry- Clean Processes and Technologies- LAQV which is financed by national funds from FCT/MEC (UID/QUI/50006/2013) and co-financed by the ERDF under the PT2020 Partnership Agreement (POCI-01-0145-FEDER-007265).

Appendix A. Supplementary material

Supplementary data associated with this article can be found in the online version at http://dx.doi.org/10.1016/j.memsci.2016.05.019.

References

[1] R.W. Baker, Concentration polarization, in: W. Baker (Ed.), Membrane Technology and Applications, John Wiley & Sons Ltd, Chichester, 2004, pp. 161–189.
[2] A. Figoli, S. Santoro, F. Galiano, A. Basile, Pervaporation membranes: preparation, characterization, and application, in: A. Basile, A. Figoli, M. Khayet (Eds.), Pervaporation, Vapour Permeation and Membrane Distillation, Principles and Applications, Woodhead Publishing, Oxford, 2015, pp. 19–63.
[3] L. Martinez-Diez, M.I. Vázquez-González, A method to evaluate coefficients affecting flux in membrane distillation, J. Membr. Sci. 173 (2000) 225–234.
[4] M. Paipuri, S. Hyeong Kim, O. Hassan, N. Hilal, K. Morgan, Numerical modelling of concentration polarisation and cake formation in membrane filtration processes, Desalination 365 (2015) 151–159.
[5] L.D. Tijing, Y.C. Woo, J.-S. Choi, S. Lee, S.-H. Kim, H.K. Shon, Fouling and its control in membrane distillation—a review, J. Membr. Sci. 475 (2015) 215–244.
[6] E.S. Tarleton, J.P. Robinson, M. Salman, Solvent-induced swelling of membranes measurements and influence in nanofiltration, J. Membr. Sci. 280 (2006) 442–451.
[7] M. Nyström, M. Mänttäri, Opportunities and challenges of real time monitoring on membrane processes, in: C. Güell, M. Ferrando, F. López (Eds.), Monitoring and Visualizing Membrane-Based Processes, WILEY-VCH Verlag GmbH & Co. KGaA, Weinheim, 2009, pp. 1–7.
[8] M.I.J. Stich, L.H. Fischer, O.S. Wolfbeis, Multiple fluorescent chemical sensing and imaging, Chem. Soc. Rev. 39 (2010) 3102–3114.
[9] R.I. Dmitriev, A.V. Zhdanov, Y.M. Nolan, D.B. Papkovsky, Imaging of neurosphere oxygenation with phosphorescent probes, Biomaterials 34 (2013) 9307–9317.
[10] V.M. Chauhan, R.H. Hopper, S.Z. Ali, E.M. King, F. Udrea, C.H. Oxley, J.W. Aylott, Thermo-optical characterization of fluorescent rhodamine B based temperature-sensitive nanosensors using a CMOS MEMS micro-hotplate, Sens. Actuators B: Chem. 192 (2014) 126–133.
[11] C. Baleizão, S. Nagl, M. Schäferling, M.N. Berberan-Santos, O.S.W. olfbeis, Dual fluorescence sensor for trace oxygen and temperature with unmatched range and sensitivity, Anal. Chem. 80 (2008) 6449–6457.
[12] P.R.N. Childs, Advances in temperature measurement, in: J.P. Hartnett, T. F. Irvine, Y.I. Cho, G.A. Greene (Eds.), Advances in Heat Transfer 36, Accademic Press, San Diego and London, 2003, pp. 111–181.
[13] R. Ramamoorthy, P.K. Dutta, S.A. Akbar, Oxygen sensors: materials, methods, designs and applications, J. Mater. Sci. 38 (2003) 4271–4282.
[14] C.D.S. Brites, P.P. Lima, N.J.O. Silva, A. Millàn, V.S. Amaral, F. Palacio, L.D. Carlos, Thermometry at the nanoscale, Nanoscale 4 (2012) 4799–4829.
[15] C. Gosse, C. Bergaud, P. Löw, Molecular probes for thermometry in microfluidic devices, in: S. Volz (Ed.), Thermal Nanosystems and Nanomaterials, Topics in Advanced Physics 118, Springer-Verlag, Berlin, 2009, pp. 301–341.
[16] P. Marek, J.J. Velasco-Veléz, T. Haas, T. Doll, G. Sadowski, Time-monitoring sensor based on oxygen diffusion in an indicator/polymer matrix, Sens. Actuators B: Chem. 178 (2013) 254–262.
[17] S.M. Grist, L. Chrostowski, K.C. Cheung, Optical oxygen sensors for applications in microfluidic cell, Culture 10 (2010) 9286–9316.
[18] A. Balaji Ganesh, T.K. Radhakrishnan, Fiber-optic sensors for the estimation of oxygen gradients within biofilms on metals, J. Opt. Lasers Eng. 46 (2008) 321–327.
[19] R. Sakaguchi, S. Kiyonaka, Y. Mori, Fluorescent sensors reveal subcellular thermal changes, Curr. Opin. Biotechnol. 31 (2015) 57–64.
[20] K. Tsukada, S. Sakai, K. Hase, H. Minamitani, Development of catheter type optical oxygen sensor and applications to bioinstrumentation, Biosens. Bioelectron. 18 (2003) 1439–1445.
[21] J.F. Gouin, F. Baros, D. Birot, J.C. André, A fibre-optic oxygen sensor for oceanography, Sens. Actuators B: Chem. 39 (1997) 401–406.
[22] X.-D. Wang, H.-X. Chen, Y. Zhao, X. Chen, X.-R. Wang, X. Chen, Optical oxygen sensors move towards colorimetric determination, TrAC Trends Anal. Chem. 29 (2010) 319–338.
[23] P. Douglas, K. Eaton, Response characteristics of thin film oxygen sensors, Pt and Pdoctaethylporphyrins in polymer films, Sens. Actuators B: Chem. 82 (2002) 200–208.
[24] O.S. Wolfbeis, Fiber Optic Chemical Sensors and Biosensors, CRC Press, Boca Raton, 1991.
[25] Y. Amao, Probes and polymers for optical sensing of oxygen, Microchim. Acta 143 (2003) 1–12.
[26] B.J. Basu, A. Thirumurugan, A.R. Dinesh, C. Anandan, K. Rajam, Optical oxygen

sensor coating based on the fluorescence quenching of a new pyrene derivative, Sens. Actuators B: Chem. 104 (2005) 15–22.
[27] Y. Amao, T. Miyashita, I. Okura, Optical oxygen sensing based on the luminescence change of metalloporphyrins immobilized in styrene-pentafluorostyrene copolymer film, Analyst 125 (2000) 871–875.
[28] R.N. Gillanders, M.C. Tedford, P.J. Crilly, R.T. Bailey, A composite thin film optical sensor for dissolved oxygen in contaminated aqueous environments, Anal. Chem. Acta 545 (2005) 189–194.
[29] Z. Wang, A.R. McWilliams, C.E.B. Evans, X. Lu, S. Chung, M.A. Winnik, I. Manners, Covalent attachment of Ru^{II}phenanthroline complexes to polythionylphosphazenes: the development and evaluation of single-component polymeric oxygen sensors, Adv. Funct. Mater. 12 (2002) 415–419.
[30] G. Liebsch, I. Klimant, O.S. Wolfbeis, Luminescence lifetime temperature sensing based on sol–gels and poly(acrylonitrile)s dyed with ruthenium metal–ligand complexes, Adv. Mater. 11 (1999) 1296–1299.
[31] L.M. Coyle, M. Gouterman, Correcting lifetime measurements for temperature, Sens. Actuators B: Chem. 61 (1999) 92–99.
[32] M.I.J. Stich, S. Nagl, O.S. Wolfbeis, U. Henne, M. Schaeferling, A. Dual Luminescent, Sensor material for simultaneous imaging of pressure and temperature on surfaces, Adv. Funct. Mater. 18 (2008) 1399–1406.
[33] C.-S. Chu, Y.-L. Lo, Ratiometric fiber-optic oxygen sensors based on sol–gel matrix doped with metalloporphyrin and 7-amino-4-trifluoromethyl coumarin, Sens. Actuators B 134 (2008) 711–717.
[34] E.J. Park, K.R. Reid, W. Tang, R.T. Kennedy, R. Kopelman, Ratiometric fiber optic sensors for the detection of inter- and intra-cellular dissolved oxygen, J. Mater. Chem. 15 (2005) 2913–2919.
[35] X. Poteau, B. MacCraith, Ratiometric sensor for dissolved oxygen in seawater, Proc. SPIE 4876 (2003) 886–893.
[36] P.J. Cywinski, A.J. Moro, S.E. Stanca, C. Biskup, G.J. Mohr, Ratiometric porphyrin-based layers and nanoparticles for measuring oxygen in biosamples, Sens. Actuator B: Chem. 135 (2009) 472–477.
[37] J.C. Jansen, K. Friess, E. Drioli, Organic vapour transport in glassy perfluoropolymer membranes: a simple semi-quantitative approach to analyze clustering phenomena by time lag measurements, J. Membr. Sci. 367 (2011) 141–151.
[38] Y.M. Corre, S. Bruzaud, J.L. Audic, Y. Grohens, Morphology and functional properties of commercial polyhydroxyalkanoates: a comprehensive and comparative study, Polym. Test. 31 (2012) 226–235.
[39] T.M. Murphy, B.D. Freeman, D.R. Paul, Physical aging of polystyrene films tracked by gas permeability, Polymer 54 (2013) 873–880.
[40] P. Roche, R. Al-Jowder, R. Narayanaswamy, J. Young, P. Scully, A novel luminescent lifetime-based optrode for the detection of gaseous and dissolved oxygen utilising a mixed ormosil matrix containing ruthenium (4,7-diphenyl-1,10-phenanthroline)$_3$Cl$_2$ (Ru.DPp), Anal. Bioanal. Chem. 386 (2006) 1245–1257.
[41] Y.-L. Lo, C.-S. Chu, J.-P. Yur, Y.-C. Chang, Temperature compensation of fluorescence intensity-based fiber-optic oxygen sensors using modified Stern–Volmer model, Sens. Actuator B: Chem. 131 (2008) 479–488.